Rhizobium induces DNA damage in *Caenorhabditis elegans* intestinal cells

Marina Kniazeva[a,b] and Gary Ruvkun[a,b,1]

[a]Department of Molecular Biology, Massachusetts General Hospital, Harvard Medical School, Boston, MA 02114; and [b]Department of Genetics, Harvard Medical School, Boston, MA 02114

Contributed by Gary Ruvkun, January 4, 2019 (sent for review September 13, 2018; reviewed by Danielle A. Garsin and Emily R. Troemel)

In their natural habitat of rotting fruit, the nematode *Caenorhabditis elegans* feeds on the complex bacterial communities that thrive in this rich growth medium. Hundreds of diverse bacterial strains cultured from such rotting fruit allow *C. elegans* growth and reproduction when tested individually. In screens for *C. elegans* responses to single bacterial strains associated with nematodes in fruit, we found that *Rhizobium* causes a genome instability phenotype; we observed abnormally long or fragmented intestinal nuclei due to aberrant nuclear division, or defective karyokinesis. The karyokinesis defects were restricted to intestinal cells and required close proximity between bacteria and the worm. A genetic screen for *C. elegans* mutations that cause the same intestinal karyokinesis defect followed by genome sequencing of the isolated mutant strains identified mutations that disrupt DNA damage repair pathways, suggesting that *Rhizobium* may cause DNA damage in *C. elegans* intestinal cells. We hypothesized that such DNA damage is caused by reactive oxygen species produced by *Rhizobium* and found that hydrogen peroxide added to benign *Escherichia coli* can cause the same intestinal karyokinesis defects in WT *C. elegans*. Supporting this model, free radical scavengers suppressed the *Rhizobium*-induced *C. elegans* DNA damage. Thus, *Rhizobium* may signal to eukaryotic hosts via reactive oxygen species, and the host may respond with DNA damage repair pathways.

C. elegans | microbiota | DNA damage | ROS | *Rhizobium*

The free-living nematode *Caenorhabditis elegans* in the laboratory feeds on *Escherichia coli*. Cultivation of *C. elegans* on a diet of *E. coli* was natural for the *E. coli* geneticists who were the pioneers of *C. elegans* research. But the native habitat of *C. elegans* is not the laboratory, and, until recently, very little was known about its natural history (1–6). For many years, *C. elegans* has been called a soil nematode, which now appears to be inaccurate. In geographically diverse areas, *C. elegans* inhabits decaying plants and fruits, which fuel the proliferation of diverse species of bacteria which *C. elegans* finds scrumptious (5, 7). Félix and coworkers have systematically characterized the bacterial species that can be cultured from the same decaying fruits that foster the growth of *C. elegans* and other nematodes (5, 7). The potential influence on *C. elegans* of these bacterial species, either individually or in reconstructed communities of bacteria, has begun to emerge (8).

Here, we show that particular species of bacteria from the *C. elegans* natural habitat tested individually as the sole food source for *C. elegans* cultivation: For example, *Rhizobium huautlense*, inhibited normal karyokinesis during postembryonic intestinal development. Our analysis based on comprehensive *C. elegans* genetics screens, and free radical exposure or free radical scavenger treatments, show that *Rhizobium* produces reactive oxygen species (ROS), which induces DNA damage in the animal intestine to in turn cause defective karyokinesis. This ROS damage is likely to cause the formation of chromosome bridges preventing the proper separation of nuclei after a cell cycle. Chemical free radical scavengers can partially suppress this *Rhizobium*-induced DNA damage. Chemical addition of reactive oxygen to an otherwise benign *E. coli* bacteria also induced such an aberrant nuclear division. Our findings provide an insight into the interactions between microbes and animal cells.

Results and Discussion

Feeding *C. elegans* on Particular Strains of Bacteria Cultured from Its Natural Habitat Causes Abnormal Intestinal Nuclei Divisions. In the laboratory, *C. elegans* is often cultivated on a diet of *E. coli* (OP50 strain) bacteria grown from a few drops of a saturated liquid overnight culture, which is spotted on nematode growth media agar plates (NGM-plates). We cultivated *C. elegans* on individual bacterial species isolated from the *C. elegans* natural habitat of rotting fruit (3, 4, 9) instead of *E. coli* and tested whether any of these strains induce the expression of GFP fusion reporter genes associated with particular developmental milestones or with stress and immunity (8). We tested these reporter genes on a cultured collection of 90 species that coinhabit rotting fruits with *C. elegans* (the JUb bacterial library) (8) (*Materials and Methods*), which have been 16s rRNA gene sequenced for classification. A *sur-5::GFP* fusion gene (10), which expresses a nuclear-localized green fluorescent protein (GFP) in all somatic cells, allows many postembryonic cell divisions that occur during larval stages of *C. elegans* to be monitored. In *C. elegans* carrying the *sur-5::GFP* fusion cultivated on benign *E. coli*, bright GFP is observed in the intestine, where 20 large round intestinal nuclei line up in a regular pattern. The number and spatial distribution of these nuclei in larvae and adults is stereotyped. At the first larval (or L1) stage, larvae hatch with 20 mononucleated

Significance

An incredible diversity of microbial species inhabit the Earth. Many new interactions of bacteria with animals are only beginning to surface. We show that feeding a worm, *Caenorhabditis elegans,* with *Rhizobium* bacteria causes failed nuclear divisions in intestinal cells. *C. elegans* mutations compromising DNA damage repair pathways and exogenous reactive oxygen species cause similar failure in intestinal nuclear divisions, suggesting that *Rhizobium* may produce reactive oxygen species. In accordance, free radical scavenger chemicals suppress the response to *Rhizobium*. We propose that *Rhizobium* induces reactive oxygen species in its encounter with *C. elegans*. Our findings provide an insight into the interactions between microbes and animal cells.

Author contributions: M.K. and G.R. designed research; M.K. performed research; M.K. analyzed data; and M.K. and G.R. wrote the paper.

Reviewers: D.A.G., The University of Texas Health Sciences Center at Houston; and E.R.T., University of California, San Diego.

The authors declare no conflict of interest.

[1]To whom correspondence should be addressed. Email: ruvkun@molbio.mgh.harvard.edu.

This article contains supporting information online at www.pnas.org/lookup/suppl/doi:10.1073/pnas.1815656116/-/DCSupplemental.

Published online February 11, 2019.

intestinal cells formed during embryogenesis, but, during the late L1 stage, a specific subset of 8 to 12 intestinal nuclei duplicate after DNA replication and divide, and these duplicated nuclei separate without cytokinesis (i.e., karyokinesis without cytokinesis), generating binucleate intestinal cells and totaling 28 to 32 nuclei by the end of the L1 stage (11) (Fig. 1 *A*–*C*). Feeding *sur-5::GFP C. elegans* with one bacterial strain at a time from the collection of 90 bacterial species revealed that representatives of *Sphingobacterium, Pseudomonas*, *Providencia*, *Rhizobium*, and other taxa change the shape and pattern of intestinal nuclei (Fig. 1*D* and *SI Appendix*, Fig. S1 and Table S1). Some intestinal nuclei were elongated or fragmented while the normally invariant separation between daughter nuclei became irregular when animals were fed on these taxa of bacteria (Fig. 1*D* and *SI Appendix*, Fig. S1).

For a detailed investigation of the unusual gut nuclei defect, we studied one of the wild bacteria isolates, a *Rhizobium*, which had the strongest karyokinesis defect (*SI Appendix*, Fig. S1 and Table S1). This *Rhizobium* species was identified with 16S rRNA gene sequencing as *Rhizobium huautlense*. Feeding *C. elegans* with other closely related *Rhizobium* species (*R. huautlense,* ATCCBAA-115; and *Rhizobium galegae,* ATCC43677) obtained from American Type Culture Collection (ATCC), as well as the closely related genus *Agrobacterium*, also showed similar intestinal karyokinesis defects, indicating that induction of an intestinal nuclear division defect is common to multiple members of the *Agrobacterium*/*Rhizobium* clade (*SI Appendix*, Fig. S1 and Table S1).

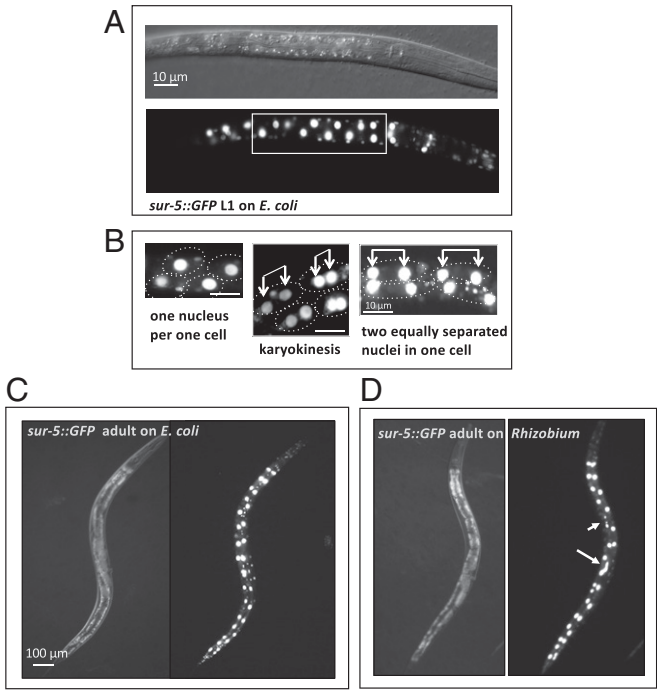

Fig. 1. Postembryonic development of *C. elegans* intestine: karyokinesis without cytokinesis during the L1 stage. (*A*) Differential interference contrast (DIC) and corresponding fluorescent images of early L1 larva with nuclei revealed by *sur-5::GFP*, which carries a nuclear localization sequence. A rectangle marks midintestinal cells that will become binucleate later during the L1 stage. (*B*) *sur-5::GFP* fluorescent images showing nuclei divisions and segregation within intestinal cells in late L1 larvae; dotted circles approximately show cell boundaries. Connected arrows point to recently divided cell nuclei. (*C*) DIC and fluorescent images of *sur-5::GFP* adult fed on *E. coli* from the time of hatching. (*D*) DIC and fluorescent images of a *sur-5::GFP* adult animal fed on *Rhizobium* from the time of hatching. Long and short arrows point to abnormally elongated and fragmented gut nuclei, respectively. On average, 78% of worms fed on *Rhizobium* have at least two instances of aberrant karyokinesis (elongated or fragmented nuclei or chromosomal bridges) whereas less than 10% have this phenotype on *E. coli* ($n > 1{,}000$).

Feeding with *Rhizobium* Disrupts Karyokinesis During Larval Stage One Intestinal Nuclei Divisions. WT *C. elegans* larvae fed with *E. coli* underwent a programmed intestinal nuclear division during the late L1 stage. These nuclei divided and moved away from each other within a cell, creating an invariant regular pattern (Figs. 1*B* and 2 *A*–*C*). In contrast, in WT larvae fed on *Rhizobium*, intestinal nuclei divided, but often failed to separate. The doublets of nuclei could be easily seen in late larvae and adults (Fig. 2 *D*–*F*). In some cases, the divided nuclei separated but remained connected with DNA bridges (Fig. 2*G*) and encapsulated in the same nuclear envelope (Fig. 2 *H*–*J*). The intestinal nuclear defects of *C. elegans* grown on *Rhizobium* were observed in 78% of animals grown on *Rhizobium* (at least two pairs of abnormal nuclei) whereas, on *E. coli*, less than 10% of the animals showed this defect. Defective intestinal karyokinesis was observed in *C. elegans* fed on *Rhizobium* from the time of hatching. The defect in karyokinesis at the L1 stage was not cured at later stages and could be easily observed in adult intestinal cells with large polyploid nuclei. If initial feeding at the L1 stage was on *E. coli* and switched to *Rhizobium* at later stages (L2 to adults), the gut nuclei pattern remained normal. Thus, the exposure to *Rhizobium* was required before DNA replication and nuclear division of intestinal cells during the late L1 stage (12). To test for inheritance of the phenotype, parent animals grown on *Rhizobium* with abnormal intestinal karyokinesis were allowed to produce progeny animals that were then fed with *E. coli* from the time of hatching, and these progeny had normal intestinal nuclei. Thus, defective intestinal karyokinesis required an exposure to the causative bacteria at early L1 larvae, and it was not inherited.

Mutations in *C. elegans* DNA Damage Response Genes also Cause Abnormal Intestinal Karyokinesis. The occurrence of chromosomal bridges and fragmented nuclei is a hallmark of DNA damage and chromosome breakage (13, 14) and suggested that such DNA damage may occur in the gut nuclei of *C. elegans* fed on *Rhizobium*. To explore what *C. elegans* processes might be affected to cause the elongated and fragmented gut nuclei, and thus reveal the host pathways that *Rhizobium* might disrupt, we mutagenized the *sur-5::GFP C. elegans* with ethyl methanesulfonate (EMS) (6) and screened two generations after the mutagenesis for *C. elegans* mutants that have elongated and fragmented gut phenotype when grown on benign *E. coli* (~10,000 haploid genomes were screened). Using whole genome sequencing, we identified point mutations in coding regions of six mutants: *atm-1* (C578T) and *dog-1* (five alleles: G759A, G118A, G845A, C346T, and splice site donor C to T between exons 6 and 7) genes (Fig. 3 and Table 1). *atm-1* encodes the *C. elegans* ortholog of ataxia telangiectasia mutated (ATM), a phosphatidylinositol 3-kinase that responds to DNA damage by phosphorylating key substrates involved in DNA repair and/or cell cycle control, and *dog-1* encodes the *C. elegans* ortholog of the helicase mutated in Fanconi anemia, also implicated in a DNA damage response. The *atm-1* and *dog-1* mutants frequently produced males, a phenotype often associated with DNA damage and aneuploidy, and were viable.

The following genetic data indicate that mutations in *atm-1* and *dog-1* genes cause the elongated gut nuclear phenotype: (*i*) Complementation tests between our isolated mutants and standard mutant alleles obtained from the Caenorhabditis Genetic Center (CGC) strain collection showed that the isolated *atm-1* and *dog-1* alleles failed to complement the standard *atm-1* and *dog-1* alleles, respectively; (*ii*) the standard CGC *atm-1* and *dog-1* mutations crossed with *sur-5::GFP* reporter showed a similar

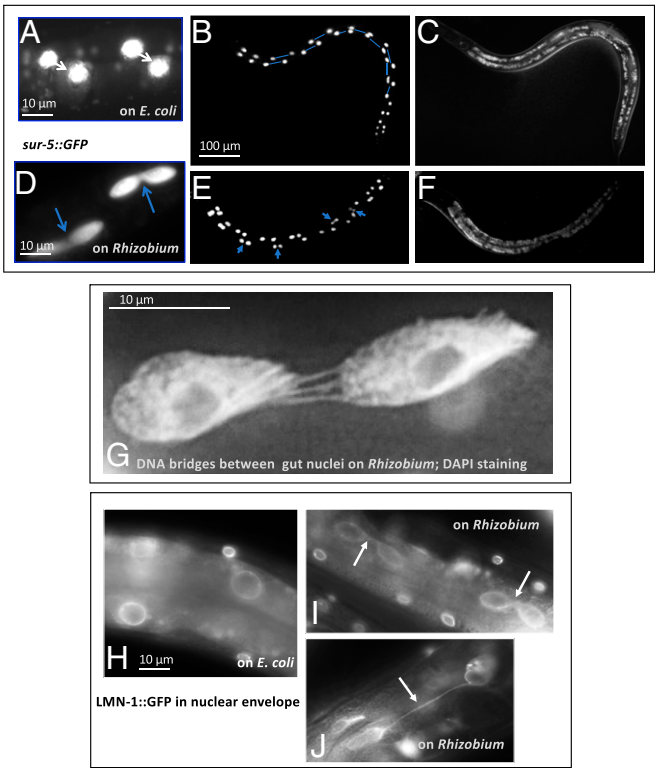

Fig. 2. In animals feeding on *Rhizobium huautlense,* intestinal nuclei divide normally during the L1 stage, but the nuclear envelopes fail to separate. (*A*–*F*) Fluorescent *sur-5::GFP* and differential interference contrast images illustrating a difference in gut nuclei segregation between *C. elegans* fed with *E. coli* (*A*–*C*) and *R. huautlense* (*D*–*F*). On *E. coli*, nuclei are evenly spaced within the binucleate intestinal cell (shown connected by lines). On *Rhizobium*, the failed segregation of nuclei is shown with arrows. (*G*) High magnification image of DAPI-stained nuclei showing multiple DNA bridges between incompletely separated intestinal nuclei in *C. elegans* fed with *Rhizobium*. (*H*) The divided intestinal nuclei highlighted by a nuclear lamin::GFP fusion protein in *C. elegans* fed with *E. coli* and nuclei failed in karyokinesis in *C. elegans* fed with *Rhizobium* (*I* and *J*). Arrows point to nuclei envelope bridges. Most of the affected animals had four to six abnormal gut nuclei randomly positioned along the intestine, out of 12 of the 20 gut cells that normally divide during the L1 stage.

karyokinesis defect (*SI Appendix*, Fig. S2 and Table S1); and (*iii*) multiple alleles of *dog-1* came out of the screen.

In all of the isolated *C. elegans* mutants, the intestinal karyokinesis defect was stronger (most of the intestinal nuclei failed to separate) and more penetrant (100% of worms, $n > 100$ were affected) (*SI Appendix*, Table S1) than in WT *C. elegans* fed *Rhizobium*. Because both genes that answered the genetic screen, *atm-1* and *dog-1*, have a role in genome stability and/or DNA damage response and repair (DDR) (15–21), this genetic analysis suggested that *C. elegans* grown on *Rhizobium* experiences DNA damage, as revealed by the *sur-5::GFP* reporter as DNA bridges and fragmented nuclei (Fig. 2).

To test if the abnormal karyokinesis phenotype is a characteristic of a specific step in the DNA damage response pathway, we performed an RNAi screen of *C. elegans* carrying *sur-5::GFP* using gene inactivation known to affect specific steps in the DNA damage response and repair pathway (22). We found that inhibition of *mus-101* (23) and *rad-51* (24) (genes representing double strand break repair pathway), *lin-40* (25) (a chromatin factor), *wwp-1* (26) (a protein degradation pathway), *nola-3* (27) (RNA processing and trafficking), and *sex-1* (28) showed abnormal gut karyokinesis similar to that observed in WT *C. elegans* grown on *Rhizobium* (*SI Appendix*, Fig. S3). Thus, the aberrant nuclei division in the gut cannot be attributed to a specific DDR gene or a single pathway. It is likely to be a consequence of general DNA damage causing compromised DNA/chromosomal integrity.

Hydrogen Peroxide Causes Intestinal DNA Damage in *C. elegans* Fed on *Rhizobium*. A common cause of DNA damage is reactive oxygen. Using a GST induction reporter gene *gst-4p::GFP* as an oxidative stress reporter (29), we showed that *C. elegans* grown on *Rhizobium*, but not on *E. coli*, induced the expression of *gst-4p::GFP* to the level comparable with the expression induced by a potent oxidizer, hydrogen peroxide (30) (Fig. 4).

How could *Rhizobium* cause oxidative stress in *C. elegans*? Using dichlorodihydrofluorescein diacetate, H2DCFDA-AM, a membrane penetrant redox detector (31, 32), we measured the

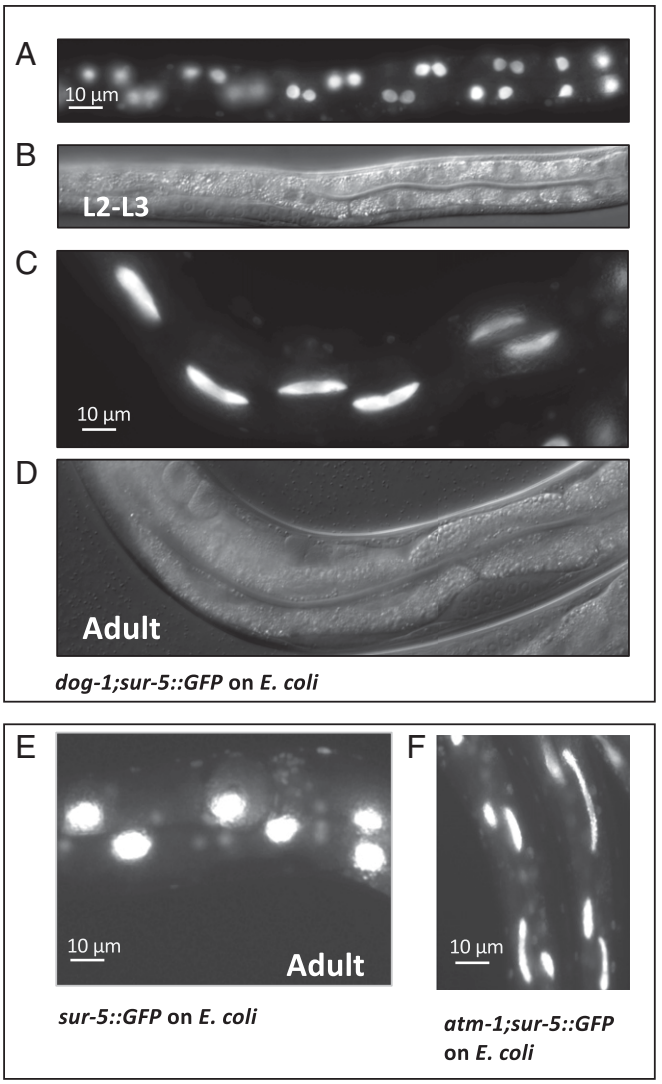

Fig. 3. *C. elegans* strains with mutations in DNA damage response pathways grown on *E. coli* show the same defective nuclear division phenotype observed in WT *C. elegans* fed with *Rhizobium huautlense*. (*A*–*D*) Fluorescence and differential interference contrast *sur-5::GFP* images of *C. elegans dog-1* mutant animals grown on *E. coli* illustrate failed intestinal nuclei segregation in L2-L3 larvae (*A* and *B*) resulting in "elongated" gut nuclei phenotype in adults (*C* and *D*). (*E* and *F*) Fluorescence images of gut nuclei patterning in *sur-5::GFP* (*E*) and the *atm-1;sur-5::GFP* adults (*F*) (one of the extreme cases). Intestinal karyokinesis is affected in 100% of *atm-1;sur-5::GFP* and *dog-1;sur-5::GFP* mutants fed with *E. coli* (*SI Appendix*, Table S1); other tissues were not evaluated.

Table 1. Mutations in the listed genes alter karyokinesis in the *C. elegans* developing intestine

Gene	Name	Cellular function	EMS mutation/ alleles	Amino acid change	CGC strains	C-test*	CGC strain gut nuclei abnormal	Human homolog
atm-1	Ataxia telangiectasia mutated family	DDR	C578T	R/C	VC381 (gk186)	No	Yes	ATM
dog-1	Deletion of G-rich DNA	DNA repair/ maintenance	G118A[†]	G/R	VC13 (gk10)	No	Yes	FANCJ/ BRIP1/ BACH1
			C15021247T position on chromosome I	Splice site donor		No		
			G759A	C/Y		n/t		
			G845A	G/D				
			C346T	P/S				

*C-test, complementation test. "No" means that a cross between the EMS mutant and the corresponding CGC strain does not rescue the abnormal phenotype, indicating that the same gene is mutated in both strains.
[†]Five alleles of *dog-1* were isolated in the screen; two were evaluated in a C-test. n/t, not tested. Amino acid abbreviations: R, arginine; C, cysteine; G, glycine; Y, tyrosine; D, aspartic acid; P, proline; S, serine. Sources: https://wormbase.org/#012-34-5.

redox status in living *Rhizobium* or *E. coli* cells (*Materials and Methods*). *Rhizobium* caused much more intense H2DCFDA-AM fluorescence than *E. coli*, indicating the presence of more oxidizing metabolites and possibly a higher level of ROS (Fig. 5 *A* and *B*). One possible source of bacterial ROS is hydrogen peroxide (H_2O_2). We measured H_2O_2 concentrations in *E. coli* and *Rhizobium* using a fluorimetric hydrogen peroxide assay. The assay utilizes a substrate for hydrogen peroxidase, an enzyme which, in the presence of hydrogen peroxide, converts it into a fluorescent compound (*Materials and Methods*). The assay is applicable for the analysis of live cells. The measurement revealed that *Rhizobium* contains about five times more hydrogen peroxide than *E. coli* (Fig. 5 *C* and *D*).

Hydrogen peroxide is cytotoxic, but highly conserved catalase enzymes protect cells by metabolizing hydrogen peroxide to water and oxygen. A simple assay can detect catalase: A drop of 3% H_2O_2 onto a freshly grown *E. coli* lawn bubbles due to oxygen production by catalase (Movies S1 and S2). A fresh *Rhizobium* lawn does not generate bubbles (Movie S3), indicating low or absent catalase activity. *C. elegans* L1 larvae exposed to 3% hydrogen peroxide on unseeded agar or on a *Rhizobium* lawn became paralyzed within minutes due to H_2O_2 toxicity. On *E. coli*, *C. elegans* larvae exposed to 3% hydrogen peroxide remained mobile. The catalase activity of *E. coli* may detoxify the H_2O_2 whereas the *Rhizobium* does not produce catalase and could not detoxify the H_2O_2 (Fig. 5 *E*–*J*). Treatment of *C. elegans* early L1 larvae with 3% hydrogen peroxide on an *E. coli* lawn induced the same defective intestinal karyokinesis as caused by *Rhizobium* feeding (Fig. 5 *K* and *L* and *SI Appendix*, Table S1): 63% of *C. elegans* fed *E. coli* and treated with 3% H_2O_2 showed defective karyokinesis.

Based on the facts that feeding on *Rhizobium*, but not *E. coli*, causes oxidative stress in *C. elegans*, that *Rhizobium* has higher cellular oxidative state and likely higher ROS than *E. coli*, that *Rhizobium* accumulate more hydrogen peroxide possibly because of low catalase activity, and that exogenous hydrogen peroxide causes intestinal karyokinesis defects similar to those induced by feeding with *Rhizobium*, we hypothesized that hydrogen peroxide produced by *Rhizobium* could be the oxidizing metabolite. *Rhizobium* could produce hydrogen peroxide in the *C. elegans* gut, the probable first *C. elegans* cells to encounter Rhizobium separated by only a cell membrane, as digestion ensues, causing, directly or indirectly, DNA damage in adjacent intestinal cells.

Hypoxia or Antioxidants Suppress the Karyokinesis Defect in *C. elegans* Grown on *Rhizobium*. If the oxidative stress model is correct, then karyokinesis defect caused by *Rhizobium* should depend on oxygen concentration. We found that hypoxia (1% oxygen) significantly reduced the defective gut karyokinesis phenotype in *C. elegans* grown on *Rhizobium* whereas high oxygen (100% oxygen) enhanced the phenotype on *Rhizobium* (graph in Fig. 6, Fig. 6 *A* and *B*, and *SI Appendix*, Table S1). Moreover, 100% O_2 caused the defective gut karyokinesis phenotype in *C. elegans* fed on normally benign *E. coli* (Fig. 6*C* and

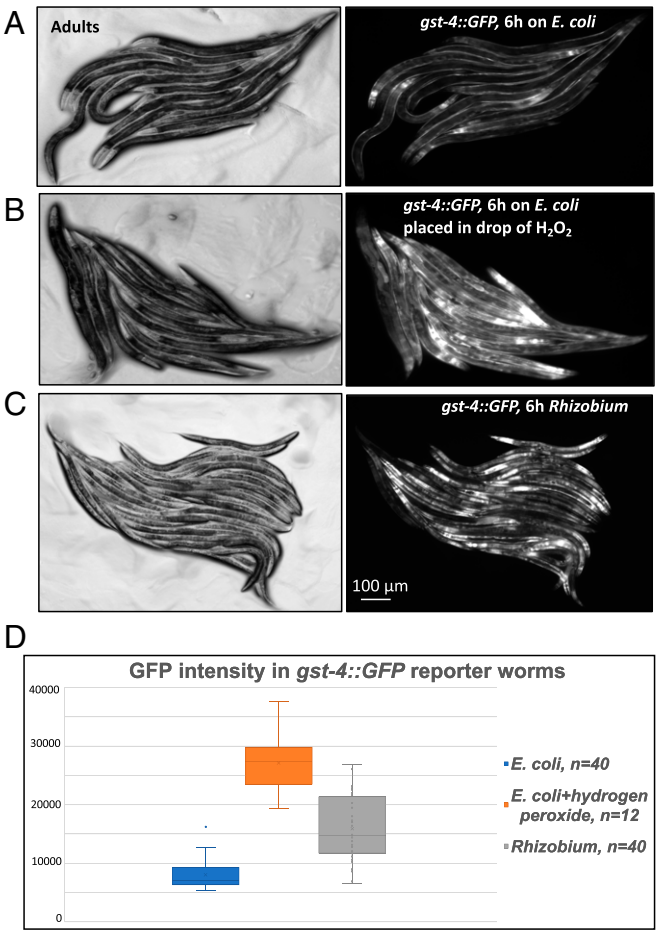

Fig. 4. Feeding on *Rhizobium* causes oxidative stress response. (*A*–*C*) Fluorescence and differential interference contrast *gst-4p::GFP* images of *C. elegans* adults transferred from an *E. coli* lawn to a new *E. coli* lawn (*A*), or transferred to a new *E. coli* lawn and treated with 30 µL of 3% H_2O_2 (*B*), or transferred to a *Rhizobium* lawn (*C*). Images were taken 6 h after the transfer of the *C. elegans*. (*D*) Graph showing the corresponding GFP intensities in the gut measured with ImageJ software. *t* test for *E. coli* vs. *E. coli* + hydrogen peroxide returns $P = 8.95503E{-}24$, and for *E. coli* vs. *Rhizobium*, $P = 1.29942E{-}12$.

MICROBIOLOGY

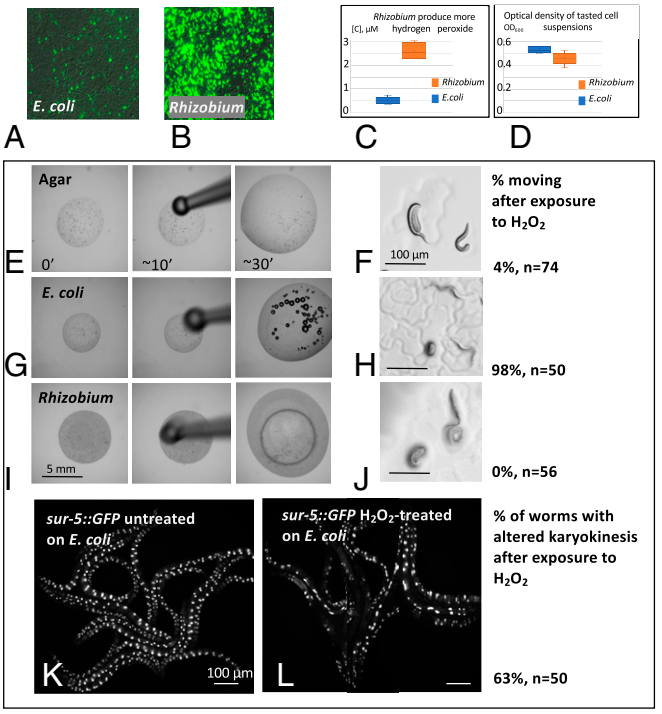

Fig. 5. *Rhizobium huautlense* cells are positive for oxidative stress, produce more hydrogen peroxide, and have less or no catalase activity. Hydrogen peroxide is sufficient to interfere with karyokinesis in the *C. elegans* gut. (*A* and *B*) A fluorescence test for oxidative stress indicates that *Rhizobium* has more redox activity (more cells have brighter fluorescence) than *E. coli* grown on NGM agar at room temperature. (*C*) A graph showing that *Rhizobium* produces more hydrogen peroxide than *E. coli* as measured by fluorimetric hydrogen peroxide assay. (*D*) Graph showing similar absorption (OD600) and therefore concentrations of *E. coli* and *Rhizobium* suspensions used in the assay. (*E*–*J*) Images of L1 larvae *C. elegans* treated with 3% hydrogen peroxide on agar (*E* and *F*), *E. coli* lawn (*G* and *H*), and *Rhizobium* lawn (*I* and *J*). Catalase activity of *E. coli* (*G* and *H*), but not *Rhizobium* (*I* and *J*) suppresses the paralysis of the L1. Numbers on the right of *F*, *H*, and *J* show percent of moving L1 larvae, and "n" is a number of scored larvae for each condition. (*K* and *L*) Fluorescence images of *sur-5::GFP* reporter *C. elegans* untreated (*K*) or treated with hydrogen peroxide (*L*) during L1 stage. Approximately 63% of treated animals developed the phenotype, $n = 50$.

SI Appendix, Table S1). These DNA damage responses to increased oxygen both on *E. coli* and *Rhizobium* are likely to be via increased production of ROS.

We tested if a treatment of L1 larvae with *N*-acetyl-cysteine (NAC), a potent antioxidant that reacts with hydrogen peroxide (33), could alleviate the *Rhizobium* gut karyokinesis defect. We treated L1 larvae with NAC by letting them hatch overnight in a solution of NAC. The treated and untreated *C. elegans* were plated on *Rhizobium* or *Rhizobium* supplemented with NAC, as well as on control *E. coli* lawns, and scored for the intestinal karyokinesis defect (*Materials and Methods*). Treatment of L1 larvae with NAC before exposure to *Rhizobium* suppressed the karyokinesis defect, but a supplementation of a *Rhizobium* lawn with NAC could not rescue the *Rhizobium*-induced karyokinesis defect in untreated larvae (*SI Appendix*, Fig. S4*A* and Table S1). The data indicate that NAC promotes a resistance to oxidative stress in larvae rather than reduced ROS levels in *Rhizobium*. These results support the hypothesis that bacterial-induced oxidative stress and ROS cause abnormal karyokinesis in intestinal nuclei.

In a related experiment, we found that growth of *C. elegans* on *Rhizobium* in the presence of an apple slice (*Materials and Methods*), likely to contain a natural antioxidant, also inhibited the intestinal karyokinesis defect (*SI Appendix*, Fig. S4*B* and Table S1). A reduction of ROS by antioxidants in the apple or indirectly through a change in *Rhizobium* metabolism is possible. The suppression of ROS damage by the apple could explain why proliferating *C. elegans* are almost always found on fallen fruits in nature, but not in soil harboring similar bacterial strains (34, 35).

***Rhizobium* Induces *C. elegans* Intestinal Karyokinesis Defects over a Short Range.** Since there were no obvious changes in karyokinesis outside of the intestine (*SI Appendix*, Fig. S5), we hypothesized that ingested *Rhizobium* disrupts intestinal karyokinesis over a short range from the lumen of the gut to the gut nucleus. We tested this hypothesis by obstructing direct contact between *Rhizobium* and *C. elegans* with a 0.22-μm-pore-size filter. The filter was placed on the *Rhizobium* lawn, and the *C. elegans* eggs were spotted on top of the filter along with a small aliquot of *E. coli* as a food to stimulate postembryonic development (36). A second filter prepared with a mixture of *E. coli* with *Rhizobium* without filter served as a control. We found that a presence of the filter between *Rhizobium* and the *C. elegans* inhibited the intestinal karyokinesis defects whereas control *C. elegans* in contact with *Rhizobium* showed the gut karyokinesis defect (*Materials and Methods* and *SI Appendix*, Fig. S6). These results suggest that the intestinal karyokinesis defect could be caused by *Rhizobium* cells contacting cells in the nematode. Such a short-range agent of DNA damage is consistent with hydrogen peroxide.

We also measured formation of 8-hydroxydeoxyguanosine (8-OHdG), one of the hallmarks of oxidative DNA damage, in chromosomal DNA isolated from *C. elegans* grown on *E. coli* and *Rhizobium* (*Materials and Methods*). We did not detect a significant difference in the concentration of 8-OHdG between the *Rhizobium*- or *E. coli*-grown *C. elegans* (*SI Appendix*, Fig. S7).

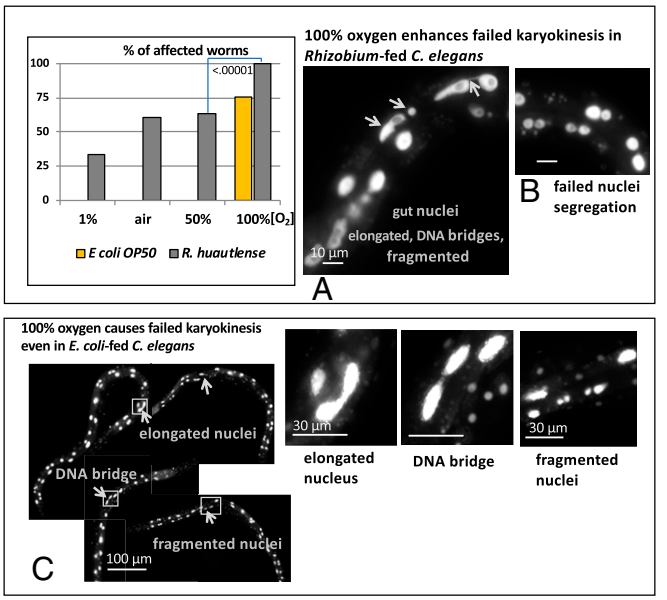

Fig. 6. Abnormal intestinal karyokinesis in *C. elegans* fed with *Rhizobium* depends on oxygen. (*A*) The graph shows the percentage of *C. elegans* with defective gut nuclear division when grown on *Rhizobium* from hatching in a chamber with indicated concentration of oxygen; $n > 50$, *P* value is shown. (*A* and *B*) Fluorescence images of gut nuclei in adult *C. elegans* fed on *Rhizobium* and maintained at 100% oxygen; (*A*) arrows point to elongated nuclei, fragmented nuclei, and nuclei connected with DNA bridges. (*B*) Closely positioned nuclei indicate a failed nuclei segregation. (*C*) Images of *C. elegans* fed with *E. coli* at 100% oxygen from the time of hatching illustrate abnormal gut nuclei pattern (arrowheads and *Insets*).

But, if DNA damage is localized to only intestinal cells (less than 1% of the DNA content of a fertile hermaphrodite), we would not expect to see a dramatic change in 8-OHdG as measured for the entire DNA content of a *C. elegans*. In published experiments, treatment of *C. elegans* with hydrogen peroxide, a known agent promoting formation of 8-OHdG (37), resulted only in a modest increase in [8-OHdG], from 20 to 25 pg per microgram of chromosomal DNA, despite high dosage of hydrogen peroxide and lengthy treatment (38). Thus, our results should not be interpreted as an absence of a change in 8-OHdG as this assay might not be sensitive enough to reveal the change in chromosomal DNA of intestinal cells.

Does Higher ROS Level Associated with Aberrant Karyokinesis in *C. elegans* Come Exclusively from Ingested *Rhizobium*? The pathogenic bacteria *Enterobacteria faecalis* does not produce ROS during infection but induces ROS production by the worm itself through activation of its dual oxidase, BLI-3 (39–41). BLI-3 has a NADPH oxidase (NOX) domain responsible for the ROS production and a peroxidase-like domain utilizing hydrogen peroxide (40, 42–44). We tested if NOX contributes to aberrant karyokinesis in worms fed on *Rhizobium*. An inhibition of NOX function in *bli-3(im10)* mutants decreases hydrogen peroxide level during *E. faecalis* infection (40). We thus crossed *bli-3 (im10)* worms with *sur-5::GFP* reporter strain and compared the karyokinesis phenotype in the worms grown on *E. coli* and *Rhizobium* (Fig. 7). The characteristic *Rhizobium*-induced elongated, double and fragmented nuclei phenotype could still be seen in these worms. This result indicated that a NOX-mediated increase in hydrogen peroxide level upon infection is not essential for the karyokinesis defect in worms grown on *Rhizobium*.

Other Phenotypes Associated with Feeding on *Rhizobium*. *C. elegans* grown on *Rhizobium* from the time of hatching were thinner and smaller in body size (*SI Appendix*, Fig. S8 *A* and *B*). We tested a hypothesis that altered karyokinesis in some intestinal cells might impair intestinal function, resulting in the body mass deficiency. We supplemented *Rhizobium* food with *E. coli* by mixing *Rhizobium* with *E. coli* 1:10, 1:1, 10:1, and 100:1 by volume and evaluated both body size and gut nuclei morphology in *C. elegans* maintained on the mixed bacterial lawns from the time of hatching. We found that supplementation with *E. coli* at any dilution fully rescued the small, scrawny phenotype, but not the intestinal karyokinesis defect, although reducing its penetrance from 79 to 40% (*SI Appendix*, Fig. S8 *C* and *D*). This result indicates that *Rhizobium* may generate less of an essential nutrient or micronutrient for rapid *C. elegans* growth that is produced by *E. coli*. Because only a small fraction of *E. coli* could suppress the slow growth phenotype, but not the intestinal karyokinesis defect, the bacterial mixing experiment also suggested that a micronutrient malnutrition rather than a gut function defect prevented normal growth in *C. elegans* fed on *Rhizobium*. Considering that the abnormal gut nuclei morphology was observed only in a few nuclei in a 1,000-celled worm, it is not surprising that the physiological consequence of it was insignificant.

A test for bacterial aversion behavior revealed that *Rhizobium* does not repel *C. elegans* (*SI Appendix*, Fig. S9), indicating that the *C. elegans* pathogen surveillance system was not activated (45). In nature, *Rhizobium* forms a symbiotic relationship with particular legumes, fixing atmospheric nitrogen for the plant in return for carbon (46, 47). The *Rhizobium*–*C. elegans* ROS interaction may be mechanistically related to this more intimate plant bacterial symbiosis.

Concluding Remarks

We have shown that the *Rhizobium* that *C. elegans* may encounter in nature in rotting fruits inhibits normal karyokinesis in intestinal cells. We could cause a similar intestinal cell phenotype via genetic lesions in *C. elegans* DNA damage response genes, *atm-1* and *dog-1*, suggesting that, indeed, DNA damage is a likely reason for abnormal nuclei divisions in the gut of *C. elegans* fed on *Rhizobium*. How does feeding on *Rhizobium* cause DNA damage in *C. elegans*? A common cause of DNA damage is reactive oxygen species (ROS). We showed that the *Rhizobium* diet evoked an oxidative stress response in *C. elegans*. A measurement of intracellular oxidative activity in *Rhizobium* revealed that it is higher than *E. coli*. The suppression of the karyokinesis defect on *Rhizobium* by growth under hypoxia conditions or with free radical scavengers also supports the model of ROS as a cause. What could be the *Rhizobium*-produced ROS? We favor the model that the ROS is hydrogen peroxide. Treatment with exogenous hydrogen peroxide causes abnormal karyokinesis similar to that caused by *Rhizobium*, and the concentration of hydrogen peroxide is higher in *Rhizobium* than in *E. coli.* In addition, it is feasible that relatively stable (half-life in milliseconds) and polar hydrogen peroxide can transit from bacteria inside the intestinal lumen, across two bacterial and one eukaryotic cell membrane, into the intestinal cell where it is converted into a hydroxyl radical in the presence of ferrous (Fe^{2+})

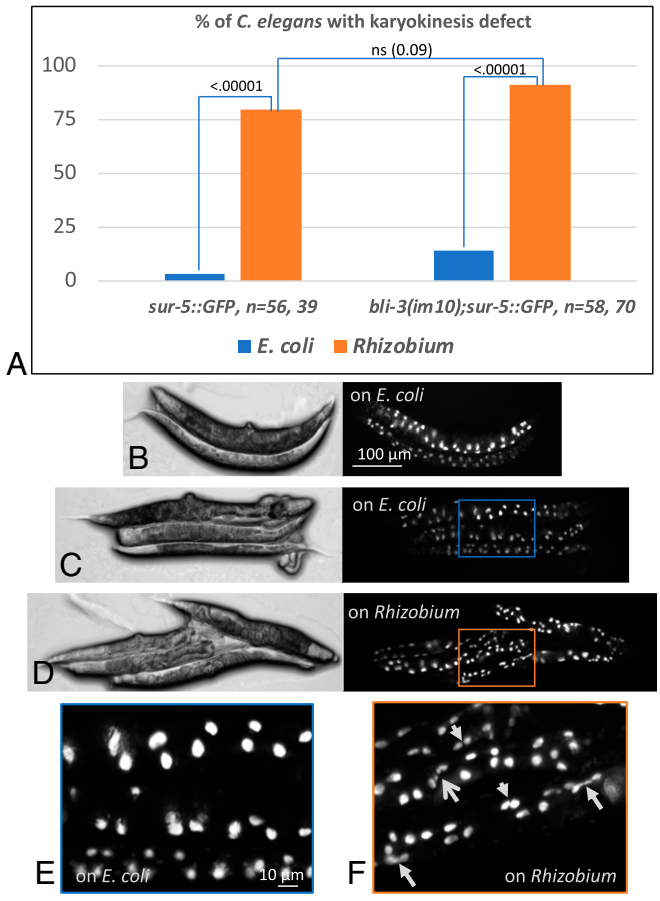

Fig. 7. Inhibition of ROS production by NOX in *bli-3(im10)* mutants does not rescue aberrant karyokinesis in gut nuclei of *C. elegans* grown on *Rhizobium*. (*A*) Graph showing percentage of worms with karyokinesis defect on *E. coli* and *Rhizobium*. *P* values are shown. ns, not significant. (*B–F*) differential interference contrast and fluorescence *bli-3(im10);sur-5::GFP* images of adult worms grown on *E. coli* (*B, C,* and *E*) and *Rhizobium* (*D* and *F*). (*E* and *F*) Enlarged *Insets* shown in *C* and *D*, correspondingly. (*F*) Arrows point to elongated (closed arrows), fragmented (open arrow), and double nuclei (short arrows). *bli-3* mutants have "blistered" phenotype and small and deformed body shapes due to its role in collagen crosslinking of the cuticle (43, 44). Because of that, the gut nuclei pattern is somewhat disturbed in comparison with WT worms but the karyokinesis defect can be observed in the intestine.

iron via the Fenton reaction (48) to damage DNA. The short half-life of this ROS would explain why a proximity between gut and *Rhizobium* cells is required for DNA damage to occur. It would also explain why most nuclei are not affected, which would be expected from a diffusion of more stable toxic product along intestinal tract. Why does the *Rhizobium* impair intestinal karyokinesis but not noticeably affect the function of the gut as might be expected from DNA damage mutagenesis? One possible explanation is that, in *C. elegans*, intestinal cells endoreduplicate genomic DNA during postembryonic development to generate the 32C per nucleus (11). The high copy number of these genomes may decrease the probability of a protein deficiency caused by DNA damage.

The altered gut nuclei phenotype is an easy readout; it could be used to further understand consequences of a high oxygen environment on animal cells. An interesting by-product of our EMS screen was a finding that the altered intestinal nuclei phenotype in *sur-5::GFP* reporter strain could be used as a discovery tool in a search for genes required for genome stability. Some of the candidate mutations selected in the screen are in the genes not previously linked to DNA damage response, repair, or chromosome segregation and, therefore, may reveal new genes involved in these processes (*SI Appendix*, Fig. S10).

In bacteria, ROS [superoxide (O_2-), hydrogen peroxide (H_2O_2), and hydroxyl ion ($HO\cdot$)] are naturally generated during aerobic growth when molecular oxygen acquires electrons from reduced cofactors of various flavoproteins (49) and from side reactions of the electron transport chain (50). ROS inhibits enzymes containing iron or iron–sulfur clusters, including multiple enzymes involved in DNA replication and repair. To resist ROS, bacteria have evolved a number of strategies, such as the ROS efflux, compartmentalization, scavenging, and DNA repair mechanisms (49, 51). Some bacteria use ROS in fighting prokaryotic competitors less protected from oxidative stress, by either releasing ROS or inducing ROS production within neighboring cells by secreting redox cycling drugs (51–56). ROS-producing *Helicobacter pylori* and *Enterococcus faecalis* in the mammalian intestine may cause double strand breaks in DNA of epithelial cells, thus contributing to gastric carcinogenesis (57, 58). Killing of *C. elegans* with streptococcal species and *Enterococcus faecium* via hydrogen peroxide has been reported (59–61). It would be fascinating to explore the potential countermeasures that eukaryotes marshal to respond to bacteria and the counter countermeasures in turn used by bacteria.

Materials and Methods

The *C. elegans* and Bacteria Strains and Maintenance. The *C. elegans* and bacteria strains and maintenance were as follows: N2 Bristol, GR3065: translational *sur-5::GFP* from laboratory stock; VC381: *atm-1(gk186)*, VC13: *dog-1(gk10)*, CL2166: *gst-4p::GFP*, GS3798: arIs99 [*dpy-7p::2Xnls::YFP*], and LW699: GFP-tagged LMN-1 were obtained from CGC; GR3066: *atp-1(mg665)*; *sur-5::GFP*, GR3067: *dog-1(mg666);sur-5::GFP*, GR3068: *dog-1(mg667);sur-5::GFP*, GR3069: *dog-1(mg668);sur-5::GFP*, GR3195: *dog-1(mg694);sur-5::GFP*, and GR3196: *dog-1(mg695);sur-5::GFP* were generated by EMS in the course of this study. *bli-3(im10)* was a gift from Hiroki Moribe, Kurume University School of Medicine, Fukuoka, Japan. These mutants were crossed with *sur-5::GFP* reporter strain. All strains were maintained at 15 °C on nematode growth media (NGM) (62) agar plates in the presence of streptomycin (250 μg/mL final concentration) and seeded with OP50-1 *E. coli* carrying an integrated streptomycin resistance gene (CGC). Throughout the text, it is referred to as *E. coli*. RNAi was performed as described (63).

The library of the wild bacterial isolates (JUb) was created by, and obtained from, the M.-A. Félix laboratory (3, 8, 64). *Rhizobium huautlense* (ATCCBAA-115) and *Rhizobium galegae* (ATCC43677) were obtained from ATCC. Agrobacterium was a gift from the Jen Sheen laboratory (Department of Molecular Biology, Massachusetts General Hospital, Harvard Medical School, Boston).

Screening the JUb Library. Bacteria were grown in liquid LB for 3 to 4 d at room temperature until suspensions appeared cloudy. Then, 300 μL of the liquid cultures were spotted on 3-cm NGM agar plates without antibiotic. The plates with the bacteria were maintained at room temperature for 2 d before setting up experiments. *C. elegans sur-5::GFP* eggs were obtained by bleaching gravid adults (62) and were spotted on the top of the bacterial lawn. The plates with *C. elegans* were maintained at 15 °C. The phenotypes were scored at various time points. Identity of all bacterial strains mentioned in this work was confirmed by 16S sequencing (MacrogenUSA).

Microscopy and DAPI Staining. For staining with DAPI, 30 *C. elegans* were transferred to a 1.5-mL Eppendorf tube filled with 20 μL of cold methanol and kept at −20 °C for 5 min. Methanol was aspirated, and 20 μL of S-basal (62) was added and pipetted up and down to separate bacteria stuck to *C. elegans*. The bacteria suspended in S-basal were removed. Finally, 10 μL of S-basal with 0.5 μL of DAPI solution (200×) was added to the worm pellet. After 5 min of incubation with DAPI, the worm's corpses were mounted on a microscopic agarose pad.

Live and fixed *C. elegans* were visualized with AxioZoom.V16 (Zeiss) and AxioImagerZ.1 (Zeiss) microscopes equipped with OrkaFlash 4.0 (Hamamatsu) and Axiocam HRc (Zeiss) cameras, respectively. Images were processed with ImageJ software.

Feeding *C. elegans* with *Rhizobium*. The *Rhizobium* cultures and plates were prepared as described above for the JUb library clones. Control *E. coli* strain was grown the same way and plated on NGM without antibiotics. Typically, two to three adults or 100 eggs or L1 larvae hatched in S-basal buffer overnight were plated on the lawns.

Testing a Requirement for a Contact Between the *Rhizobium* and *C. elegans* for Inducing Intestinal Nuclei Phenotype. A small, 10-mm-diameter, *Rhizobium* lawn was covered with a polyethersulfone (PES) 0.2-μm, 25-mm membrane filter (Sterlitech Corp.). Then, 100 μL of overnight suspension of *E. coli*, was placed on the top of the filter and was allowed to form a lawn. This was needed to stimulate the worm's development, which requires consumption of the live bacterial food (36). As a control, 100 μL of LB without *E. coli* was added to the *Rhizobium* lawn and to the *Rhizobium* covered with the filter. Analogously, 100 μL of *E. coli* was added to the *Rhizobium* lawn without the filter. Bleached *sur-5::GFP* eggs were plated on the top. The gut phenotype was scored in the grown adults ($n = 50$).

EMS Mutagenesis and Selection of Mutants. Mutagenesis of *sur-5::GFP* was done according to the published protocol (6). The aliquots of treated *C. elegans* were distributed on dozens of 10-cm NGM agar plates seeded with 10× concentrated *E. coli* bacterial lawn. Second generation (F1) progeny were bleached and plated in aliquots on 10 10-cm NGM agar plates seeded with 10× concentrated *E. coli* bacterial lawn. Adults (F2) with the desired phenotype were cloned, and homozygote progeny were outcrossed with a parental strain more than two times. Fewer than 10,000 haploid genomes were screened; the screen was not performed to saturation.

Identification of EMS mutants.

Next-generation sequencing of EMS mutants. DNA isolation, library construction, and whole genome sequencing with Illumina were carried out according to the published protocol (65).

Complementation test. Available alleles of the candidate genes were obtained from CGC and crossed with corresponding EMS mutants. An appearance of the altered gut nuclei phenotype indicated failed complementation and suggested that corresponding genes are the causative genes.

Evaluation of the gut nuclei phenotype with* sur-5::GFP *reporter. The candidate mutants obtained from CGC were outcrossed two times and crossed with *sur-5::GFP*, and their gut nuclei phenotype was evaluated on *E. coli* bacterial lawn.

RNAi Screen. *C. elegans sur-5::GFP* adults were bleached, and eggs were plated on bacterial lawn expressing RNAi (63) targeting a subset of DDR genes. Adult *C. elegans* were evaluated for abnormal gut nuclei.

Oxidative Stress Detection in *E. coli* and *Rhizobium* with H2DCFDA-AM Reagent. The reagent dichlorodihydrofluorescein diacetate allowed the oxidative stress detection inside living cells. The procedure was according to the provided protocol: 10 μL of H2DCFDA-AM reagent (Molecular Probes) [10× stock solution in DMSO] spotted on the top of bacterial lawns. After 1 h at room temperature, cells were transferred on microscopic agarose and evaluated under the UV scope.

Hydrogen Peroxide Detection in *E. coli* and *Rhizobium*. Bacteria were grown in LB liquid media at room temperature to saturation ($OD_{600} \sim 0.5$). The suspensions were spun down and resuspended in the same volume of S-basal media. Then, 50 μL of the suspension in triplicates were tested for hydrogen peroxide concentration with a Fluorimetric Hydrogen Peroxide Assay Kit according to the manufacturer's protocol (Sigma-Aldrich). Fluorescence Ex λ540/Em λ590 was measured with microplate reader SpectraMax M5[e] (Molecular Dynamics).

Hydrogen Peroxide Treatment. Early L1 larvae hatched in S-basal overnight were spotted on the small (~1 cm in diameter) *E. coli* lawn on regular NGM plates. Then, 50 μL of 3% hydrogen peroxide was added so that all of the lawn area was covered. An appearance of bubbles (oxygen) indicated the presence of hydrogen peroxide and catalase activity: $2H_2O_2 \rightarrow \text{catalase} \rightarrow 2H_2O+O_2$. The plates were kept at room temperature. The adult *C. elegans* grown from the treated L1 were inspected on day 3.

Catalase Tests. To test catalase activity, 10 μL of 3% hydrogen peroxide was dropped on *E. coli* and *Rhizobium* lawns; a generation of bubbles was observed and recorded. To test the efficiency of bacterial catalase on reducing hydrogen peroxide concentration, 5 μL of synchronized L1 larvae in S-basal were plated on agar, *E. coli* and *Rhizobium* lawns and immediately covered with hydrogen peroxide at a toxic dose of 30 μL of 3%. The process and generation of bubbles on *E. coli*, but not on agar or *Rhizobium*, was recorded. Two hours later, the *C. elegans* were visually examined for their ability to move.

Oxygen Treatment. *Rhizobium* and *E. coli* lawns on NGM plates without antibiotics prepared as described above were seeded with *C. elegans* eggs and placed in oxygen chambers (Hypoxia Incubator Chamber; Stemcell technologies) with 1% (hypoxia) and high oxygen (50% and 100%) at 20 °C and kept under the conditions for 2 d. The phenotype was scored in adults.

Evaluation of DNA Damage with 8-OHdG ELISA. Chromosomal DNA was extracted from adult *C. elegans* grown on *E. coli* and *Rhizobium* according to the manufacturer's protocol (Puregene Tissue kit; Qiagen). Isolated DNA was treated with nuclease P1 and shrimp alkaline phosphatase (Sigma-Aldrich) to prepare for the assay as instructed in the protocol (OxiSelect Oxidative DNA Damage ELISA Kit; Cell Biolabs). Three biological replicates (DNA isolated from different batches of *C. elegans* on different days) and two technical replicates (split DNA solution from the same isolate) were obtained from *C. elegans* grown on *E. coli* and two biological and two technical replicates from the *C. elegans* grown on *Rhizobium*. The samples and standards were treated according to the protocol (OxiSelect Oxidative DNA Damage ELISA Kit; Cell Biolabs). Microplate reader SpectraMax M5[e] (Molecular Dynamics) was used for measurement absorption at 450 nm. Concentration of 8-hydroxydeoxyguanosine (8-OHdG) in the samples was determined according to the standard curve in Excel.

Treating *C. elegans* with *N*-acetyl-cysteine. Stock solution of NAC (Sigma-Aldrich) was prepared by dissolving 80 mg of NAC crystals in 10 mL of sterile water (~50 mM). Then, 1 mL of NAC solution or sterile water (as a control) was added on the top of 3-d-old *E. coli* or *Rhizobium* lawn on NGM agar without antibiotics, making roughly 5 mM final concentration of NAC. Eggs obtained by bleaching were spotted immediately after addition of NAC or water to the plates. Also, NAC (1/10 by volume) was added to the rest of the egg prep and incubated overnight at room temperature. L1 larvae hatched in NAC solution were plated on the *E. coli* and *Rhizobium* plates treated with NAC as above. Adult *C. elegans* were scored for the abnormal gut nuclei phenotype.

Feeding *C. elegans* with an Apple Supplement. *Rhizobium* plates were prepared as described above. Red apple cultivars, MacIntosh and Macoun, obtained from a local grocery store, were tested. The apples were wiped out with ethanol-soaked paper and rinsed with sterile water three times. Apple slices were cut out with a sterile blade and placed on the top of bacterial lawn. *C. elegans* eggs were plated on the top and near the slices (one slice per plate). No contaminating bacteria or fungi were visually detected on the apple plates within 5 to 6 d of the experiment.

Statistics. Whenever applicable, the experiments were done at least in three biological triplicates with 50 to 100 *C. elegans* at each condition when not indicated otherwise. *P* values were calculated with *t* test using Excel (Microsoft office) or calculating *z* score for the difference between two datasets.

ACKNOWLEDGMENTS. We thank members of the G.R. laboratory for helpful discussions; the Marie-Anne Félix group for sharing a collection of wild bacterial isolates; the Jen Sheen laboratory for the gift of Agrobacteria; and the Caenorhabditis Genetics Center (CGC) for providing worm strains. The work was supported by NIH Grants GM044619 and AG043184 (to G.R.).

1. Shtonda BB, Avery L (2006) Dietary choice behavior in Caenorhabditis elegans. *J Exp Biol* 209:89–102.
2. MacNeil LT, Watson E, Arda HE, Zhu LJ, Walhout AJM (2013) Diet-induced developmental acceleration independent of TOR and insulin in C. elegans. *Cell* 153: 240–252.
3. Frézal L, Félix M-A (2015) C. elegans outside the Petri dish. *eLife* 4:381.
4. Schulenburg H, Félix M-A (2017) The natural biotic environment of *Caenorhabditis elegans*. *Genetics* 206:55–86.
5. Dirksen P, et al. (2016) The native microbiome of the nematode Caenorhabditis elegans: Gateway to a new host-microbiome model. *BMC Biol* 14:38.
6. Brenner S (1974) The genetics of Caenorhabditis elegans. *Genetics* 77:71–94.
7. Félix M-A, Braendle C (2010) The natural history of Caenorhabditis elegans. *Curr Biol* 20:R965–R969.
8. Samuel BS, Rowedder H, Braendle C, Félix M-A, Ruvkun G (2016) Caenorhabditis elegans responses to bacteria from its natural habitats. *Proc Natl Acad Sci USA* 113: E3941–E3949.
9. Félix M-A, et al. (2013) Species richness, distribution and genetic diversity of Caenorhabditis nematodes in a remote tropical rainforest. *BMC Evol Biol* 13:10.
10. Gu T, Orita S, Han M (1998) Caenorhabditis elegans SUR-5, a novel but conserved protein, negatively regulates LET-60 Ras activity during vulval induction. *Mol Cell Biol* 18:4556–4564.
11. Hedgecock EM, White JG (1985) Polyploid tissues in the nematode Caenorhabditis elegans. *Dev Biol* 107:128–133.
12. Sulston JE, Horvitz HR (1977) Post-embryonic cell lineages of the nematode, Caenorhabditis elegans. *Dev Biol* 56:110–156.
13. Dass Singh M, et al. (2017) Infant birth outcomes are associated with DNA damage biomarkers as measured by the cytokinesis block micronucleus cytome assay: The DADHI study. *Mutagenesis* 32:355–370.
14. Bakhoum SF, Kabeche L, Compton DA, Powell SN, Bastians H (2017) Mitotic DNA damage response: At the crossroads of structural and numerical cancer chromosome instabilities. *Trends Cancer* 3:225–234.
15. Jones MR, Huang JC, Chua SY, Baillie DL, Rose AM (2012) The atm-1 gene is required for genome stability in Caenorhabditis elegans. *Mol Genet Genomics* 287:325–335.
16. Youds JL, et al. (2008) DOG-1 is the Caenorhabditis elegans BRIP1/FANCJ homologue and functions in interstrand cross-link repair. *Mol Cell Biol* 28: 1470–1479.
17. Saito TT, Lui DY, Kim H-M, Meyer K, Colaiácovo MP (2013) Interplay between structure-specific endonucleases for crossover control during Caenorhabditis elegans meiosis. *PLoS Genet* 9:e1003586.
18. Liu J, et al. (2000) Isolation of C. elegans and related nematodes. *Mol Biol Cell* 11: 3937–3947.
19. Hopson S, Thompson MJ (2017) BAF180: Its roles in DNA repair and consequences in cancer. *ACS Chem Biol* 12:2482–2490.
20. Liu J, et al. (2000) Essential roles for Caenorhabditis elegans lamin gene in nuclear organization, cell cycle progression, and spatial organization of nuclear pore complexes. *Mol Biol Cell* 11:3937–3947.
21. Shimada K, et al. (2013) TORC2 signaling pathway guarantees genome stability in the face of DNA strand breaks. *Mol Cell* 51:829–839.
22. van Haaften G, et al. (2006) Identification of conserved pathways of DNA-damage response and radiation protection by genome-wide RNAi. *Curr Biol* 16:1344–1350.
23. Holway AH, Hung C, Michael WM (2005) Systematic, RNA-interference-mediated identification of mus-101 modifier genes in Caenorhabditis elegans. *Genetics* 169: 1451–1460.
24. Takanami T, Mori A, Takahashi H, Horiuchi S, Higashitani A (2003) Caenorhabditis elegans Ce-rdh-1/rad-51 functions after double-strand break formation of meiotic recombination. *Chromosome Res* 11:125–135.
25. Solari F, Bateman A, Ahringer J (1999) The Caenorhabditis elegans genes egl-27 and egr-1 are similar to MTA1, a member of a chromatin regulatory complex, and are redundantly required for embryonic patterning. *Development* 126:2483–2494.
26. Carrano AC, Liu Z, Dillin A, Hunter T (2009) A conserved ubiquitination pathway determines longevity in response to diet restriction. *Nature* 460:396–399.
27. Camon E, et al. (2003) The gene ontology annotation (GOA) project: Implementation of GO in SWISS-PROT, TrEMBL, and InterPro. *Genome Res* 13:662–672.
28. Carmi I, Kopczynski JB, Meyer BJ (1998) The nuclear hormone receptor SEX-1 is an X-chromosome signal that determines nematode sex. *Nature* 396:168–173.
29. Tawe WN, Eschbach ML, Walter RD, Henkle-Dührsen K (1998) Identification of stress-responsive genes in Caenorhabditis elegans using RT-PCR differential display. *Nucleic Acids Res* 26:1621–1627.
30. Imlay JA, Chin SM, Linn S (1988) Toxic DNA damage by hydrogen peroxide through the Fenton reaction in vivo and in vitro. *Science* 240:640–642.
31. LeBel CP, Ischiropoulos H, Bondy SC (1992) Evaluation of the probe 2′,7′-dichlorofluorescin as an indicator of reactive oxygen species formation and oxidative stress. *Chem Res Toxicol* 5:227–231.

32. Kalyanaraman B, et al. (2012) Measuring reactive oxygen and nitrogen species with fluorescent probes: Challenges and limitations. *Free Radic Biol Med* 52:1–6.
33. Aruoma OI, Halliwell B, Hoey BM, Butler J (1989) The antioxidant action of N-acetylcysteine: Its reaction with hydrogen peroxide, hydroxyl radical, superoxide, and hypochlorous acid. *Free Radic Biol Med* 6:593–597.
34. Berg M, et al. (2016) Assembly of the Caenorhabditis elegans gut microbiota from diverse soil microbial environments. *ISME J* 10:1998–2009.
35. Barrière A, Félix MA (2006) Isolation of C. elegans and related nematodes. *WormBook,* 1–9.
36. Qi B, Kniazeva M, Han M (2017) A vitamin-B2-sensing mechanism that regulates gut protease activity to impact animal's food behavior and growth. *eLife* 6:781.
37. Takeuchi T, Nakajima M, Morimoto K (1996) Relationship between the intracellular reactive oxygen species and the induction of oxidative DNA damage in human neutrophil-like cells. *Carcinogenesis* 17:1543–1548.
38. Aan GJ, Zainudin MSA, Karim NA, Ngah WZW (2013) Effect of the tocotrienol-rich fraction on the lifespan and oxidative biomarkers in Caenorhabditis elegans under oxidative stress. *Clinics (São Paulo)* 68:599–604.
39. Chávez V, Mohri-Shiomi A, Garsin DA (2009) Ce-Duox1/BLI-3 generates reactive oxygen species as a protective innate immune mechanism in Caenorhabditis elegans. *Infect Immun* 77:4983–4989.
40. van der Hoeven R, Cruz MR, Chávez V, Garsin DA (2015) Localization of the dual oxidase BLI-3 and characterization of its NADPH oxidase domain during infection of Caenorhabditis elegans. *PLoS One* 10:e0124091.
41. Hoeven Rv, McCallum KC, Cruz MR, Garsin DA (2011) Ce-Duox1/BLI-3 generated reactive oxygen species trigger protective SKN-1 activity via p38 MAPK signaling during infection in C. elegans. *PLoS Pathog* 7:e1002453.
42. Chávez V, Mohri-Shiomi A, Maadani A, Vega LA, Garsin DA (2007) Oxidative stress enzymes are required for DAF-16-mediated immunity due to generation of reactive oxygen species by Caenorhabditis elegans. *Genetics* 176:1567–1577.
43. Edens WA, et al. (2001) Tyrosine cross-linking of extracellular matrix is catalyzed by Duox, a multidomain oxidase/peroxidase with homology to the phagocyte oxidase subunit gp91phox. *J Cell Biol* 154:879–891.
44. Moribe H, et al. (2012) Tetraspanin is required for generation of reactive oxygen species by the dual oxidase system in Caenorhabditis elegans. *PLoS Genet* 8:e1002957.
45. Melo JA, Ruvkun G (2012) Inactivation of conserved C. elegans genes engages pathogen- and xenobiotic-associated defenses. *Cell* 149:452–466.
46. Ruvkun GB, Sundaresan V, Ausubel FM (1982) Directed transposon Tn5 mutagenesis and complementation analysis of Rhizobium meliloti symbiotic nitrogen fixation genes. *Cell* 29:551–559.
47. Arthikala M-K, et al. (2014) RbohB, a Phaseolus vulgaris NADPH oxidase gene, enhances symbiosome number, bacteroid size, and nitrogen fixation in nodules and impairs mycorrhizal colonization. *New Phytol* 202:886–900.
48. Walling C (2002) Fenton's reagent revisited. *Acc Chem Res* 8:125–131.
49. Imlay JA (2013) The molecular mechanisms and physiological consequences of oxidative stress: Lessons from a model bacterium. *Nat Rev Microbiol* 11:443–454.
50. Boveris A (1977) Mitochondrial production of superoxide radical and hydrogen peroxide. *Tissue Hypoxia and Ischemia*, Advances in Experimental Medicine and Biology (Springer US, Boston), pp 67–82.
51. Seaver LC, Imlay JA (2004) Are respiratory enzymes the primary sources of intracellular hydrogen peroxide? *J Biol Chem* 279:48742–48750.
52. Kohanski MA, Dwyer DJ, Hayete B, Lawrence CA, Collins JJ (2007) A common mechanism of cellular death induced by bactericidal antibiotics. *Cell* 130:797–810.
53. Bienert GP, Schjoerring JK, Jahn TP (2006) Membrane transport of hydrogen peroxide. *Biochim Biophys Acta* 1758:994–1003.
54. Hawes SE, et al. (1996) Hydrogen peroxide-producing lactobacilli and acquisition of vaginal infections. *J Infect Dis* 174:1058–1063.
55. Pericone CD, Overweg K, Hermans PW, Weiser JN (2000) Inhibitory and bactericidal effects of hydrogen peroxide production by Streptococcus pneumoniae on other inhabitants of the upper respiratory tract. *Infect Immun* 68:3990–3997.
56. St Amant DC, Valentin-Bon IE, Jerse AE (2002) Inhibition of Neisseria gonorrhoeae by Lactobacillus species that are commonly isolated from the female genital tract. *Infect Immun* 70:7169–7171.
57. Huycke MM, Abrams V, Moore DR (2002) Enterococcus faecalis produces extracellular superoxide and hydrogen peroxide that damages colonic epithelial cell DNA. *Carcinogenesis* 23:529–536.
58. Handa O, Naito Y, Yoshikawa T (2011) Redox biology and gastric carcinogenesis: The role of Helicobacter pylori. *Redox Rep* 16:1–7.
59. Jansen WTM, Bolm M, Balling R, Chhatwal GS, Schnabel R (2002) Hydrogen peroxide-mediated killing of Caenorhabditis elegans by Streptococcus pyogenes. *Infect Immun* 70:5202–5207.
60. Bolm M, Jansen WTM, Schnabel R, Chhatwal GS (2004) Hydrogen peroxide-mediated killing of Caenorhabditis elegans: A common feature of different streptococcal species. *Infect Immun* 72:1192–1194.
61. Moy TI, Mylonakis E, Calderwood SB, Ausubel FM (2004) Cytotoxicity of hydrogen peroxide produced by Enterococcus faecium. *Infect Immun* 72:4512–4520.
62. Stiernagle T (2006) Maintenance of C. elegans. *WormBook,* 1–11.
63. Kamath RS, Ahringer J (2003) Genome-wide RNAi screening in Caenorhabditis elegans. *Methods* 30:313–321.
64. Félix M-A, Duveau F (2012) Population dynamics and habitat sharing of natural populations of Caenorhabditis elegans and C. briggsae. *BMC Biol* 10:59.
65. Lehrbach NJ, Ji F, Sadreyev R (2017) Next-generation sequencing for identification of EMS-induced mutations in Caenorhabditis elegans. *Curr Protoc Mol Biol* 117:7.29.1–7.29.12.